Table 3 Histological feature comparison between echinoderm microtubule-associated protein-like-4—anaplastic lymphoma kinase (EML4-ALK)-positive and -negative lung adenocarcinoma

		EML4-ALK (+)	EML4-ALK (−)	p Value*
Extra- and/or intra-cytoplasmic mucin production	(+)	6	30	0.0001
	(−)	2	216	
Cribriform pattern with extracytoplasmic mucin	(+)	5	8	<0.0001
	(−)	3	238	
Signet-ring cell appearance	(+)	1	4	0.149
	(−)	7	242	

*Fisher's exact test.

EML4-ALK-negative lung cancers.[5 6 10 15] In this study EML4-ALK-positive lung adenocarcinoma was less differentiated, as described in a previous report.[6] However, EML4-ALK-positive and -negative lung adenocarcinomas showed no difference in age, sex, tumour size, smoking habit and TNM stage. The screening was limited in this study to lung adenocarcinomas of Japanese patients. Previous reports showed that lung cancers harbouring the EML4-ALK fusion gene were mostly adenocarcinomas with a few exceptions.[10 15] All EML4-ALK-positive lung adenocarcinomas had no mutation in the EGFR and KRAS genes, which concurred with previous reports.[6 9 15]

A previous report revealed the association of EML4-ALK fusion and acinar-predominant morphology[9] and signet-ring cell appearance.[5 10] In this study, acinar-predominant morphology and cribriform pattern with excessive extracytoplasmic mucin were useful factors, suggesting the presence of the EML4-ALK fusion gene, but signet-ring cell appearance by itself was not a useful factor. Previous reports revealed an association of EML4-ALK fusion and signet-ring cell appearance. However, the subjects screened were in a Western population or with limited clinical characteristics.[5 10] There may be an underlying difference in the subject population by race and clinical characteristics. A recent report showed that primary signet-ring cell carcinoma of the lung shares many clinicopathologic characteristics with EML4-ALK-positive lung cancers.[16] In point of fact, one case of EML4-ALK-positive lung adenocarcinoma in our study had signet-ring cell appearance. However, because the population of tumour cells appearing like signet-ring cells was very low, it was not a useful independent factor, suggesting the presence of the EML4-ALK fusion gene. It may however, be a clue in suggesting the presence of the EML4-ALK fusion gene because of excessive mucin production.

Previous reports have shown the utility of immunohistochemistry for EML4-ALK.[11 12] Our study showed the usefulness of characteristic morphological features in screening for EML4-ALK-positive lung adenocarcinomas. The combined study of typical morphological features of EML4-ALK-positive lung adenocarcinomas by light microscopy followed by immunohistochemical confirmation may enable the screening for EML4-ALK-positive lung adenocarcinomas to be simple and cost effective.

Although light microscopic observations of specific morphological features and immunohistochemistry are very useful, two of our eight EML4-ALK-positive cases did not have characteristic morphological features. The two cases showed acinar-

Table 4 Clinical features of echinoderm microtubule-associated protein-like-4—anaplastic lymphoma kinase (EML4-ALK)-positive lung adenocarcinoma

Case no.	Age (y)	Sex	Smoking habit	Tumour size (mm)*	EGFR mutation	KRAS mutation	Lymph node metastasis	pStage	Prognosis
1	46	F	Never	16	(−)	(−)	Negative	IA	AN (11 mth)
2	64	M	Ever	45	(−)	(−)	Negative	IB	Recurrence at 12 mth alive (23 mth)
3	44	M	Ever	25	(−)	(−)	Positive (pN2)	IIIA	Recurrence at 29 mth alive (42 mth)
4	67	F	Never	28	(−)	(−)	Positive (pN1)	IIA	Recurrence at 20 mth alive (39 mth)
5	60	F	Ever	28	(−)	(−)	Negative	IA	AN (15 mth)
6	77	M	Ever	25	(−)	(−)	Negative	IA	AN (11 mth)
7	67	F	Unknown	10	(−)	(−)	Positive (pN2)	IIIA	DD (12 mth)
8	69	M	Ever	30	(−)	(−)	Positive (pN1)	IIA	DD (43 mth)

*Size is represented by the maximum width of the neoplasm.
AN indicates patient is alive with no evidence of disease; DD, died from disease; acinar, acinar adenocarcinoma; papillary, papillary adenocarcinoma; mixed, adenocarcinoma with mixed subtypes.
pStage, pathological stage; EGFR, epidermal growth factor receptor.

Table 5 Pathological features of echinoderm microtubule-associated protein-like-4—anaplastic lymphoma kinase (EML4-ALK)-positive lung adenocarcinoma

Case no.	WHO subtype	Predominant subtype	Minor component subtypes	ALK positive tumour cells (%)	Mucin production	Cribriform pattern	Signet-ring cell appearance
1	Mixed	Acinar	Papillary	100	(+)	(+)	(−)
2	Mixed	Papillary	Acinar	90	(+)	(+)	(−)
3	Acinar	Acinar	–	100	(+)	(+)	(−)
4	Acinar	Acinar	–	80	(+)	(+)	(−)
5	Mixed	Acinar	Solid	100	(+)	(−)	(+)
6	Mixed	Papillary	BAC, acinar, micropapillary	100	(+)	(+)	(−)
7	Acinar	Acinar	–	100	(−)	(−)	(−)
8	Acinar	Acinar	–	100	(−)	(−)	(−)

Mixed indicates adenocarcinoma with mixed subtypes; acinar, acinar adenocarcinoma; papillary, papillary adenocarcinoma; mixed, adenocarcinoma with mixed subtypes; solid, solid adenocarcinoma with mucin production; BAC, bronchioloalveolar carcinoma, non-mucinous; micropapillary, micropapillary carcinoma; mucin production, extra- and/or intra-cytoplasmic mucin production; histological pattern, specific histological pattern; cribriform, cribriform pattern with excessive extracytoplasmic mucin; signet-ring cell, signet-ring cell appearance.

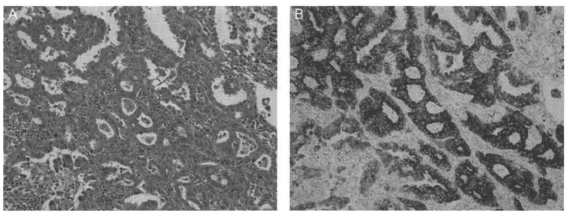

Figure 4 (A) One echinoderm microtubule-associated protein-like-4—anaplastic lymphoma kinase (EML4-ALK)-positive lung adenocarcinoma showing acinar pattern without mucin production. (B) ALK protein was expressed in the cytoplasm with no nuclear stain.

Take-home messages

- EML4-ALK-positive lung adenocarcinomas were significantly less differentiated than the EML4-ALK-negative lung adenocarcinomas.
- EML4-ALK-positive lung adenocarcinomas showed significant associations with intra- and/or extra-cytoplasmic mucin, and cribriform pattern with excessive extracytoplasmic mucin.
- The combined study of typical morphological features of EML4-ALK-positive lung adenocarcinomas by light microscopy followed by immunohistochemical confirmation may enable the screening for EML4-ALK-positive lung adenocarcinomas to be simple and cost effective.

predominant morphology but no mucin production (figure 4 and table 5). A large-scale, multi-institute study will be needed to offer more insight into EML4-ALK-positive lung adenocarcinomas.

In this study, the FISH assay was performed only on positive cases. Standard methods are not yet established for detection of the EML4-ALK fusion gene in lung cancers. As previous reports showed,[5 17] both FISH and immunohistochemistry may have false negative results. However, to perform the FISH assay on all screening cases at any institute is a costly undertaking. Immunohistochemistry, on the other hand, has been used widely in the diagnostic laboratory. It is easy to perform and relatively inexpensive. Recently, immunohistochemistry for ALK has shown almost equal sensitivity to that of the FISH assay for the detection of EML4-ALK-positive lung adenocarcinomas.[11] In addition, the ALK fusion genes are recently discovered oncogenes in lung cancers. Conceivably, there is an unknown fusion partner of ALK, which cannot be detected by the FISH assay. Therefore, immunohistochemistry appears to be an appropriate screening method in the diagnostic laboratory.

In conclusion, we showed that EML4-ALK-positive lung adenocarcinomas had a tendency for expressing a characteristic morphological pattern. Continued investigations await the validation of the results presented in this study with respect to the potential usefulness of morphological analysis and immunohistochemistry in screening for EML4-ALK lung adenocarcinomas.

Acknowledgements The authors thank Drs Eiichi Morii and Ayumi Furumoto for helpful advice and discussion, and Mr Michihiko Noguchi, Ms Ayumi Tsukiyama, Mr Yasuhiro Hashimoto, Ms Kumi Tanaka and Ms Saori Fukuda for technical assistance.

Competing interests None.

Ethics approval This study was conducted with the approval of the ethics committee of Osaka Police Hospital.

Provenance and peer review Not commissioned; externally peer reviewed.

REFERENCES

1. **Paez JG,** Janne PA, Lee JC, *et al*. EGFR mutations in lung cancer: correlation with clinical response to gefitinib therapy. *Science* 2004;**304**:1497–500.
2. **Lynch TJ,** Bell DW, Sordella R, *et al*. Activating mutations in the epidermal growth factor receptor underlying responsiveness of non-small-cell lung cancer to gefitinib. *N Engl J Med* 2004;**350**:2129–39.
3. **Soda M,** Choi YL, Enomoto M, *et al*. Identification of the transforming EML4-ALK fusion gene in non-small-cell lung cancer. *Nature* 2007;**448**:561–6.
4. **Horn L,** Pao W. EML4-ALK: honing in on a new target in non-small-cell lung cancer. *J Clin Oncol* 2009;**27**:4232–5.
5. **Rodig SJ,** Mino-Kenudson M, Dacic S, *et al*. Unique clinicopathologic features characterize ALK-rearranged lung adenocarcinoma in the western population. *Clin Cancer Res* 2009;**15**:5216–23.
6. **Inamura K,** Takeuchi K, Togashi Y, *et al*. EML4-ALK lung cancers are characterized by rare other mutations, a TTF-1 cell lineage, an acinar histology, and young onset. *Mod Pathol* 2009;**22**:508–15.
7. **Takeuchi K,** Choi YL, Soda M, *et al*. Multiplex reverse transcription-PCR screening for EML4-ALK fusion transcripts. *Clin Cancer Res* 2008;**14**:6618–24.
8. **Rikova K,** Guo A, Zeng Q, *et al*. Global survey of phosphotyrosine signaling identifies oncogenic kinases in lung cancer. *Cell* 2007;**131**:1190–203.
9. **Inamura K,** Takeuchi K, Togashi Y, *et al*. EML4-ALK fusion is linked to histological characteristics in a subset of lung cancers. *J Thorac Oncol* 2008;**3**:13–17.
10. **Shaw AT,** Yeap BY, Mino-Kenudson M, *et al*. Clinical features and outcome of patients with non-small-cell lung cancer who harbor EML4-ALK. *J Clin Oncol* 2009;**27**:4247–53.
11. **Mino-Kenudson M,** Chirieac LR, Law K, *et al*. A novel, highly sensitive antibody allows for the routine detection of ALK-rearranged lung adenocarcinomas by standard immunohistochemistry. *Clin Cancer Res* 2010;**16**:1561–71.
12. **Takeuchi K,** Choi YL, Togashi Y, *et al*. KIF5B-ALK, a novel fusion oncokinase identified by an immunohistochemistry-based diagnostic system for ALK-positive lung cancer. *Clin Cancer Res* 2009;**15**:3143–9.
13. **Nagai Y,** Miyazawa H, Huqun, *et al*. Genetic heterogeneity of the epidermal growth factor receptor in non-small cell lung cancer cell lines revealed by a rapid and sensitive detection system, the peptide nucleic acid-locked nucleic acid PCR clamp. *Cancer Res* 2005;**65**:7276–82.
14. **Tam IY,** Chung LP, Suen WS, *et al*. Distinct epidermal growth factor receptor and KRAS mutation patterns in non-small cell lung cancer patients with different tobacco exposure and clinicopathologic features. *Clin Cancer Res* 2006;**12**:1647–53.
15. **Wong DW,** Leung EL, So KK, *et al*. The EML4-ALK fusion gene is involved in various histologic types of lung cancers from nonsmokers with wild-type EGFR and KRAS. *Cancer* 2009;**115**:1723–33.
16. **Ou SH,** Ziogas A, Zell JA. Primary signet-ring carcinoma (SRC) of the lung: a population-based epidemiologic study of 262 cases with comparison to adenocarcinoma of the lung. *J Thorac Oncol* 2010;**5**:420–7.
17. **Martelli MP,** Sozzi G, Hernandez L, *et al*. EML4-ALK rearrangement in non-small cell lung cancer and non-tumor lung tissues. *Am J Pathol* 2009;**174**:661–70.

Human Cancer Biology
See commentary p. 4909

Clinical Cancer Research

EML4-ALK Fusion Gene Assessment Using Metastatic Lymph Node Samples Obtained by Endobronchial Ultrasound-Guided Transbronchial Needle Aspiration

Yuichi Sakairi[1,7], Takahiro Nakajima[1,2,7], Kazuhiro Yasufuku[2], Dai Ikebe[3], Hajime Kageyama[4], Manabu Soda[5], Kengo Takeuchi[6], Makiko Itami[3], Toshihiko Iizasa[1], Ichiro Yoshino[7], Hiroyuki Mano[5], and Hideki Kimura[1]

Abstract

Purpose: Anaplastic lymphoma kinase (*ALK*) fusion genes represent novel oncogenes for non–small cell lung cancers (NSCLC). Several *ALK* inhibitors have been developed, and are now being evaluated in *ALK*-positive NSCLC. The feasibility of detecting *ALK* fusion genes in samples obtained by endobronchial ultrasound-guided transbronchial needle aspiration (EBUS-TBNA) was determined. The clinicopathologic characteristics of *ALK*-positive lung cancer were also analyzed.

Experimental Design: From April 2008 to July 2009, NSCLC cases with hilar/mediastinal lymph node metastases detected by EBUS-TBNA were enrolled. Positive expression of *ALK* fusion protein was determined using immunohistochemistry, and *ALK* gene rearrangements were further examined to verify the translocation between *ALK* and partner genes using fluorescent *in situ* hybridization and reverse transcription-PCR. Direct sequencing of PCR products was performed to identify *ALK* fusion variants.

Results: One hundred and nine cases were eligible for the analysis using re-sliced samples. Screening of these specimens with immunohistochemistry revealed *ALK* positivity in seven cases (6.4%), all of which possessed echinoderm microtubule–associated protein-like 4–*ALK* fusion genes as detected by fluorescent *in situ* hybridization and reverse transcription-PCR. All *ALK*-positive cases had an adenocarcinoma histology and possessed no *EGFR* mutations. Compared with *ALK*-negative cases, *ALK*-positive cases were more likely to have smaller primary tumors ($P < 0.05$), to occur at a younger age (<60 years; $P < 0.05$), and to occur in never/light smokers (smoking index < 400; $P < 0.01$). Mucin production was frequently observed in *ALK*-positive adenocarcinomas (29.4%; $P < 0.01$).

Conclusions: EBUS-TBNA is a practical and feasible method for obtaining tissue from mediastinal and hilar lymph nodes that can be subjected to multimodal analysis of *ALK* fusion genes in NSCLC. *Clin Cancer Res; 16(20); 4938–45. ©2010 AACR.*

A small inversion within the short arm of human chromosome 2 leads to the generation of a fusion gene between the anaplastic lymphoma kinase (*ALK*) gene and the echinoderm microtubule–associated protein-like 4 (*EML4*) gene, the protein product of which is reported to function as an oncokinase in non–small cell lung cancer (NSCLC); in fact, this was the first oncogenic translocation to be identified in lung cancer (1). The *EML4-ALK* fusion gene has been detected in ~5% of NSCLC cases, and several *ALK* fusion gene variants have been reported (2). Standard methods for the detection of *ALK* fusion genes include reverse transcription-PCR (RT-PCR) with primers flanking the fusion points, as well as fluorescent *in situ* hybridization (FISH). Previously, immunohistochemistry-based diagnosis of *ALK* fusion genes in lung cancer has proven to be difficult, most likely due to the low expression level of the fusion protein products (3). An intercalated antibody-enhanced polymer (iAEP) technique has recently been developed that enables reliable immunohistochemistry-based detection of *ALK* fusion products (4). However, this technique has only been performed in cell lines and in large, surgically resected specimens; thus, it remains unclear whether such methodology can be applied to small biopsy samples obtained from patients with advanced NSCLC.

Endobronchial ultrasound-guided transbronchial needle aspiration (EBUS-TBNA) is an established modality for the definitive diagnosis of mediastinal and hilar adenopathy in

Authors' Affiliations: [1]Division of Thoracic Diseases, Chiba Cancer Center, Chiba, Japan; [2]Division of Thoracic Surgery, Toronto General Hospital, University Health Network, University of Toronto, Canada; [3]Division of Surgical Pathology, Chiba Cancer Center, Chiba, Japan; [4] Division of Genetic Diagnosis, Chiba Cancer Center, Chiba, Japan; [5]Division of Functional Genomics, Jichi Medical University, Tochigi, Japan; [6]Division of Pathology, The Cancer Institute, Japanese Foundation for Cancer Research, Tokyo, Japan; and [7]Department of General Thoracic Surgery, Graduate School of Medicine, Chiba University, Chiba, Japan

Corresponding Author: Takahiro Nakajima, Division of Thoracic Diseases, Chiba Cancer Center, 666-2 Nitona-cho, Chuo-ku 260-8717, Chiba, Japan. Phone: 81-43-264-5431; Fax: 81-43-262-8680; E-mail: nakajii@fc.med.miyazaki-u.ac.jp.

doi: 10.1158/1078-0432.CCR-10-0099

Translational Relevance

Acquisition of proper tissue samples for molecular analysis is not always an easy task; however, information obtained from such specimens is essential for the selection of appropriately targeted cancer therapies. This study shows that endobronchial ultrasound-guided transbronchial needle aspiration (EBUS-TBNA) contributes to the resolution of this issue in lung cancer because tissue samples obtained by EBUS-TBNA can be successfully used to assess the presence of echinoderm microtubule–associated protein-like 4–anaplastic lymphoma kinase fusion genes. We have shown that EBUS-TBNA samples could be subjected to immunohistochemistry, fluorescent *in situ* hybridization, and reverse transcription-PCR analysis. EBUS-TBNA for the assessment of mediastinal and hilar adenopathy is a practical tool that can be used in the molecularly targeted treatment era for lung cancer.

patients with lung cancer (5, 6). EBUS-TBNA is generally accepted to be as safe as standard bronchoscopy, less invasive than mediastinoscopy, and of high diagnostic quality. Compared with conventional fine-needle aspiration, EBUS-TBNA is an outstanding procedure with respect to its extremely low morbidity and its repeatability; fine-needle aspiration could cause pneumothorax, and repeated sampling might be difficult to perform.

In this study, we analyzed the feasibility of EBUS-TBNA for the detection of *EML4-ALK* fusion genes. We also retrospectively analyzed the clinicopathologic characteristics of *ALK*-positive lung cancer cases with mediastinal and/or hilar lymph node metastasis.

Materials and Methods

Patients

From April 2008 to July 2009, 112 cases with proven hilar and/or mediastinal lymph node metastasis of NSCLC were enrolled; re-sliced specimens for histologic examination were available for 109 of these cases. Independent pathologists (D. Ikebe and M. Itami) reviewed all cases and histologically confirmed the presence of cancer cells in each specimen. Morphologic features detected with H&E staining were also recorded, and mucin production was evaluated by Alcian blue staining. First, samples were screened for *ALK* abnormalities using immunohistochemistry. Cases that were determined to be *ALK*-positive or suspicious by immunohistochemistry in our laboratory were subjected to additional evaluation by FISH and immunohistochemistry restaining by an independent pathologist (K. Takeuchi) at the Division of Pathology, The Cancer Institute, Japanese Foundation for Cancer Research. Final confirmation was performed by direct sequencing of *EML4-ALK* fusion cDNAs using EBUS-TBNA histologic cores that had been preserved at −80°C. *EGFR* gene mutation status was also evaluated in all EBUS-TBNA samples. Associations between the presence of *ALK* fusion genes and clinicopathologic characteristics were retrospectively analyzed from medical records.

EBUS-TBNA

In all cases, chest computed tomography was performed prior to EBUS-TBNA. Brain magnetic resonance imaging, enhanced computed tomography, and bone scintigraphy were also performed for clinical staging of each case. EBUS-TBNA was performed for lymph nodes >5 mm in short axis on chest computed tomography. To obtain a histologic core, a dedicated 22-gauge needle equipped with an internal stylet was used. After the initial puncture, the internal stylet was used to clean out the internal lumen that was clogged with bronchial tissue (Fig. 1A). The internal stylet was removed, and negative pressure was applied using a syringe. The needle was then moved back and forth inside the lymph node. Finally, the needle was retrieved, and the internal stylet was used to push out the histologic core (6). Each histologic core was divided into two samples: one was fixed with formalin and used for histologic diagnosis, and the other was mixed with Allprotect Tissue Reagent (Qiagen) following the instructions of the manufacturer, and stored at −80°C.

ALK detection with immunohistochemistry

For detection of the *ALK* fusion gene, we applied the iAEP method, which incorporates an intercalating antibody between the primary antibody to *ALK* and dextran polymer–based detection reagents (4).

Histologic cores obtained by EBUS-TBNA were routinely fixed in 20% neutralized formalin and embedded in paraffin. Blocks were sliced at a thickness of 4 μm, and sections were placed on silane-coated slides. Antibody preparations specific for the intracellular region of *ALK* (5A4, Abcam) were subjected to immunohistochemical staining according to standard protocols using dextran polymer reagents (anti-mouse immunoglobulin, EnVision+DAB System; Dako). The *ALK* antibody (5A4) was used at a dilution of 1:50. For antigen retrieval and deparaffinization, slides were heated for 20 minutes at 98°C in Target Retrieval Solution (low pH; Dako) with PT-link (Dako). Pretreated slides were positioned in a programmable AutoStainer instrument (EnVision System; Dako). Following the immunohistochemical program, slides were incubated at room temperature first with Peroxidase Blocking Solution (Dako) for 5 minutes and then with *ALK* antibody (5A4, 1:50; Abcam) for 30 minutes. Following application of the iAEP method, which has been described in detail elsewhere (4), we included an incubation step of 15 minutes at room temperature with intercalated immunoglobulin (Mouse-LINKER; Dako) to increase the detection sensitivity. Immune complexes were then detected using the dextran polymer reagent for 30 minutes. 5A4-positive cells were stained with 3,3′-diaminobenzidine for 5 minutes, and nuclei were then stained with hematoxylin for 2 minutes.

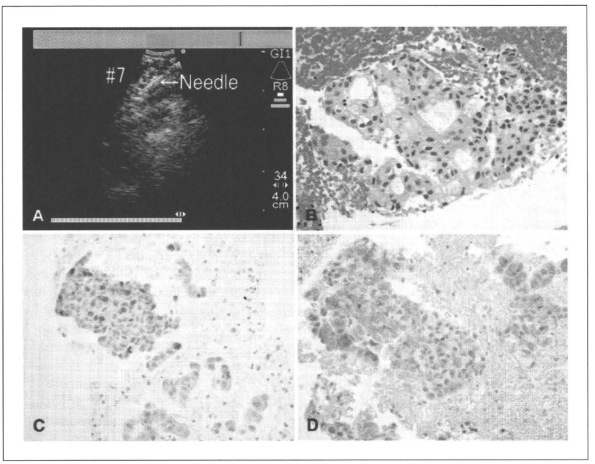

Fig. 1. Diagnosis of metastatic nodes by EBUS-TBNA. A, lymph node sampling by EBUS-TBNA. B, adenocarcinoma was revealed in the EBUS-TBNA sample. C, mucin production was observed by Alcian blue staining. D, immunohistochemistry with an anti-*ALK* antibody showed *ALK* fusion protein positivity in lung adenocarcinoma cells.

The samples obtained with EBUS-TBNA were small, paraffin-embedded biopsy specimens, which might limit the utility of immunohistochemistry. To avoid false-negative diagnosis, the first immunohistochemical procedure was used as a screening test to define three categories with which to judge the first run. Cancer cells were defined as "positive" if staining was as strongly positive as a positive control (clinical lung cancer tissues previously defined as positive by both molecular and immunohistochemistry analyses) and a fine, granular cytoplasmic staining pattern was observed. Cancer cells that showed no staining were classified as "negative." The "suspicious" classification was defined as the presence of weakly stained cells that were considered difficult to differentiate from background staining. While using these categories, we further subdivided the suspicious category into "probably positive" and "probably negative" categories. Probably positive meant that the tumor cells stained, but not strongly, whereas probably negative indicated very weak staining that was difficult to differentiate from background staining. After the screening immunohistochemistry, suspicious cases were re-tested by immunohistochemistry in addition to FISH by a second independent pathologist (K. Takeuchi).

Fluorescence *in situ* hybridization

To further confirm the *ALK* genomic rearrangement, two FISH assays were performed: an *ALK* split assay and an *EML4-ALK* fusion assay. Unstained sections were processed with a Histology FISH Accessory Kit (Dako), subjected to hybridization with fluorescently-labeled bacterial artificial chromosome clone probes for *EML4* and *ALK* (self-produced probes; *EML4* RP11-996L7, *ALK* RP11-984I21, and RP11-62B19) or for genomic regions upstream and downstream of the *ALK* breakpoint (Dako), stained with 4,6-diamidino-2-phenylindole, and examined with a fluorescence microscope (BX51; Olympus; ref. 7). FISH analysis was performed at the Division of Pathology, The Cancer Institute, Japanese Foundation for Cancer Research (K. Takeuchi). The FISH positivity criteria for EBUS-TBNA samples were defined as "over 50% cancer cells." As EBUS-TBNA samples are small biopsy samples, entire tumor cells in the paraffin-embedded section were evaluated.

RT-PCR and direct sequencing

Frozen histologic cores obtained by EBUS-TBNA were used to extract RNA. All immunohistochemistry-positive or suspicious cases were subjected to direct sequencing of the fusion cDNAs. RNA was extracted from frozen samples using the AllPrep DNA/RNA mini kit (Qiagen), and cDNA cloning was performed with the High Capacity RNA-to-cDNA Kit (Applied Biosystems). For RT-PCR analysis of *EML4-ALK*, we used primer sequences that have been described previously (2). After PCR amplification, PCR products were analyzed using agarose gel electrophoresis. RT-PCR products were extracted from gel slices using the QIAquick Gel Extraction Kit (Qiagen). Purified products were then sequenced with a capillary sequencer. Resultant nucleotide sequences were compared with previously reported sequences for determination of the *EML4-ALK* variant. *EGFR* mutation status was also examined using the peptide nucleic acid/locked nucleic acid PCR clamp method for samples obtained with EBUS-TBNA (8).

Ethics committee approval

This research was approved by the Ethics Committee of Chiba Cancer Center (nos. 20-21 and 21-10). Written consent was obtained from all patients. All samples were coded and managed independently.

Statistical analysis

For clinical characteristics and genetic factors, frequency analysis was performed with Fisher's exact test (dichotomous factors) and χ^2 test (multinomial factors). Mann-Whitney *U* test was applied to continuous data. General data analysis was conducted with StatView 5.0 (SAS Institute, Inc.). All *P* values were based on a two-sided hypothesis, $P < 0.05$ was considered to have statistical significance.

Results

Patient characteristics

The clinical characteristics of all 109 patients are listed in Table 1; 82 patients (75.2%) were male. The median age was 64.4 years (range, 38–90 y). Histologic examination was performed in all cases, leading to a diagnosis of adenocarcinoma (Fig. 1B) in 82 cases (75.2%), squamous cell carcinoma in 18 cases, and "other" in 9 cases. With respect to smoking status, 22 cases (20.4%) were never-smokers, 15 (13.9%) were light smokers (defined as a smoking index score <400), and 72 were heavy smokers (smoking index score ≥400). A total of 191 mediastinal lymph nodes and 84 hilar lymph nodes (2.52 lymph nodes/patient) were detected with EBUS, and 158 mediastinal lymph nodes and 71 hilar lymph nodes (2.10 lymph nodes/patient) were sampled. The median size of the sampled lymph nodes was 12.1 mm (range, 3.0–33.4 mm) in the short axis on ultrasound. According to criteria from the International Union Against Cancer, there were 9 stage II cases, 49 stage III cases, and 45 stage IV cases; the remaining 6 cases were defined as having recurrent lung cancer. *EGFR* gene mutations were detected in 25 cases (22.9%), which included 9 cases with in-frame deletions at exon 19, 9 cases with a point mutation at exon 21, 3 cases with a point mutation at exon 18, 2 cases with point mutations at exons 18 and 21, 1 case with a point mutation at exon 20, and 1 case with point mutations in exons 20 and 21.

Table 1. Clinical characteristics of patients with NSCLC

Parameter	Number of cases (%)
	109
Age	
Mean (y)	64.4 (range, 38–90)
Gender	
Male	82 (75.2%)
Female	27 (24.8%)
Pathology	
Adenocarcinoma	82 (75.2%)
Squamous cell	18 (16.5%)
Other histology	9 (8.3%)
Clinical stage	
II	9 (8.3%)
III	49 (45.0%)
IV	45 (41.3%)
Recurrence	6 (5.5%)
Bone metastasis	
Yes	22 (20.2%)
No	87 (79.8%)
Brain metastasis	
Yes	16 (14.7%)
No	93 (85.3%)
Smoking	
Never (SI = 0)	22 (20.4%)
Light (SI < 400)	15 (13.9%)
Heavy (SI ≥ 400)	70 (64.8%)
EGFR mutation status	25 (22.9%)
Exon 18	3
Exon 19	9
Exon 20	1
Exon 21	9
Exons 18 + 21	2
Exons 20 + 21	1

Abbreviation: SI, smoking index.

ALK fusion gene assessment

Out of 109 cases examined by immunohistochemistry using the iAEP method, 6 *ALK*-positive cases and 17 suspicious cases (1 probably positive and 16 probably negative) cases were detected. The staining of the small histologic core did not show any heterogeneity.

FISH confirmed the existence of an *ALK* fusion gene in all six *ALK*-positive cases (Figs. 1D, 2A and B), and there were no false-positive cases for immunohistochemistry. Sixteen probably negative cases were determined to be negative for the *ALK* fusion gene by re-testing with immunohistochemistry and FISH. One probably positive case had too few tumor cells to be used for FISH analysis; however, RT-PCR assessment confirmed the presence of *EML4-ALK* fusion cDNA. *EML4*, *ALK*, and fusion signals (arrows in Fig. 2A) are presented in the green, red, and merged image and a pair of split signals (arrow in Fig. 2B, downstream) shows rearrangement of *ALK*. In Fig. 2C, unique bands in each *ALK*-positive case reveal variant 1 and variant 3 *EML4-ALK* fusion genes. Thus, the *ALK* fusion gene was detected in a total of seven cases (6.4%). Direct sequencing of the PCR products revealed that four cases carried *EML4-ALK* variant 1, whereas three cases had variant 3. The fusion point of *ALK* and *EML4* is observed in the cDNA sequence (arrow in Fig. 2D).

Clinicopathologic characteristics of lung cancers possessing *ALK* fusion genes

Clinicopathologic characteristics were compared between the 7 *ALK*-positive cases and the 102 *ALK*-negative

cases (Table 2). All *ALK*-positive cases had an adenocarcinoma histology and lacked *EGFR* gene mutations. With respect to smoking habits, six out of the seven *ALK*-positive cases were either never-smokers or light smokers (smoking index score <400). No significant difference in gender was observed between *ALK*-positive and *ALK*-negative patients; however, *ALK*-positive patients were significantly younger than *ALK*-negative patients (55.4 versus 65.0 years; $P = 0.0408$). No significant differences in the incidence of bone metastasis (9.1% versus 5.7%; $P = 0.64$) or brain metastasis (12.5% versus 5.4%; $P = 0.30$) were observed. Overall, the mean primary tumor diameter was 40.4 mm; interestingly, the mean primary tumor diameter of *ALK*-positive cases was 28.6 mm, which was significantly smaller than that of *ALK*-negative cases (41.9 mm; $P < 0.05$). Mucin production was significantly more frequently observed in *ALK*-positive cases as shown by Alcian blue staining (Fig. 1C; $P < 0.01$). Finally, among the 84 cases expressing wild-type *EGFR*, 8.3% (7 of 84) were *ALK*-positive.

Discussion

This is the first attempt and report about using EBUS-TBNA samples in the detection of *ALK* fusion genes, and is expected to have a major effect on the management of patients with lung cancer. EBUS-TBNA is an established procedure for the evaluation of mediastinal and hilar adenopathy in patients with lung cancer. It is as safe, as highly diagnostic, and less invasive than other diagnostic modalities (9–11). Biopsy samples obtained with EBUS-TBNA can be subjected to histologic as well as cytologic evaluation. Nonsurgical modalities for obtaining tumor specimens are particularly critical in lung cancer because many patients have advanced disease at the time of first presentation, and are therefore not eligible for radical surgery. In addition to histologic diagnosis and stage definition, EBUS-TBNA enables molecular analysis of biopsy samples, the clinical significance of which is growing as molecularly targeted strategies for NSCLC are becoming increasingly important. We have previously reported that metastatic lymph node samples obtained by EBUS-TBNA can be applied to multidisciplinary analyses (5), and the present study is the first report of successful analysis of *ALK* fusion genes, a newly identified genetic abnormality in NSCLC, with such specimens (2). However, the small size of the paraffin-embedded biopsy samples obtained from EBUS-TBNA might limit the utility of this methodology; thus, multidirectional analysis will be critical for microsampling methods such as EBUS-TBNA.

The reliability of the newly developed immunohistochemistry (iAEP) method for the detection of *ALK* fusion

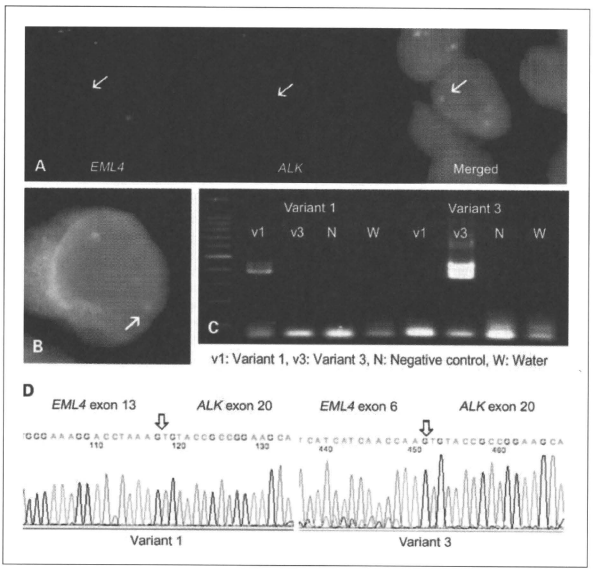

Fig. 2. Molecular analysis of *ALK* fusion genes. A, FISH *EML4-ALK* fusion assay with labeled probes for *EML4* (green, arrow) or *ALK* (red, arrow). The *EML4-ALK* fusion gene is observed (yellow, arrow). B, *EML4-ALK* split assay with labeled probes for the upstream (red) or downstream (green, arrow) region of the *ALK* locus. C, RT-PCR detection of the *EML4-ALK* fusion gene. D, direct cDNA sequence of *EML4-ALK* variants 1 and 3.

Table 2. Clinical, pathologic, and genetic analysis of *ALK*-positive NSCLC

Characteristic	*EML4-ALK* fusion			*P*
	NSCLC	+	–	
Female gender	27	4	23	0.062
Mean age (y)	64.4	55.4	65.0	0.0408
<60	29	5	24	0.0139
Bone metastasis	22	2	20	0.6396
Brain metastasis	16	2	14	0.2973
Mean tumor diameter (mm)	40.4	28.6	41.9	0.0478
Smoking index (n = 107)	784	161	827	0.0071
Never/light smoker	37	6	31	0.0056
Adenocarcinoma	82	7	75	0.1896
Mucin production	17	5	12	0.0009
EGFR wild-type	84	7	77	0.3317
ALK variant 1		4		
ALK variant 3		3		

NOTE: Two cases without primary tumors and six cases of recurrence were excluded from the tumor diameter analysis. Smoking history was recorded in 107 patients.

genes is very precise (4). This method is expected to be more practical for the detection of *ALK* fusion genes compared with FISH because FISH can sometimes be very difficult to perform for *ALK* fusion genes due to the close proximity of the two fusion gene components. We performed both fusion and split assays for FISH, and FISH was performed to confirm the immunohistochemical results. In addition, the *ALK* fusion genes are novel oncogenes in lung cancer. There is a possibility of existing unknown fusion pattern which cannot be detected by FISH or RT-PCR. Immunohistochemistry has an advantage of detecting novel unknown fusion patterns (4). In this study, we performed immunohistochemistry using the iAEP methodology and an Autostainer instrument. This technique is convenient, highly reproducible, and enables accurate diagnosis even if only a small amount of specimen is available. These features are well-suited for the screening of *ALK*-positive lung cancers using small biopsy samples. The Autostainer instrument also allows uniform immunohistochemical analysis, which may lead to consistent results among different institutions/hospitals; such uniformity is essential for the standardization of diagnostic procedures that assess the presence of *ALK* fusion genes. Recently, a highly sensitive antibody directed against *ALK* fusion products that can possibly be used for immunohistochemistry has been reported, therefore representing a novel candidate for *ALK* fusion detection (12).

The median age of *ALK*-positive cases in the present study was 55.4 years. Patients <60 years represent approximately 10% of all lung cancer deaths (6,655 of 63,255 deaths) according to the Japanese National Cancer Center Cancer Information Service Statistics published in 2008 (13). In the present study, a significant number of *ALK*-positive cases were <60 years of age (17.2%, 5 of 29; $P < 0.05$). *ALK*-positive cancer may therefore be more common in patients with early-onset NSCLC. However, it should be noted that two *ALK*-positive cases were >70 years of age (71 and 73 years); therefore, although patient age may become a predictor of *ALK* fusion gene positivity, *ALK* screening must also be performed in elderly individuals. The median diameter of primary lung tumors was significantly smaller in *ALK*-positive cases (28.6 versus 41.9 mm; $P < 0.05$), further emphasizing the importance of EBUS-TBNA because this technique does not require a large primary lesion. An additional advantage of EBUS-TBNA is that it can be used for lymph node sampling, which is relevant to the majority of advanced lung cancer cases. Although lung cancer is generally more common in smokers, most of the *ALK*-positive cases in this study (37 cases; 34.3%) were never-smokers or light smokers. The smoking index scores in the *ALK*-positive cohort were significantly lower than that of *ALK*-negative patients (161 versus 827; $P < 0.01$). Hence, being a never-smoker or light smoker seems to be a strong predictor of *ALK* positivity ($P < 0.01$).

Evaluation of the clinicopathologic characteristics of patients in our cohort indicated that *ALK*-positive lung cancer tends to have an adenocarcinoma histology, expresses wild-type *EGFR*, has an early age of onset (<60 y), manifests as a relatively small primary lesion, more frequently occurs in never-smokers or light smokers (smoking index score <400), and has a mucin-producing histology. However, as EBUS-TBNA samples are obtained from metastatic lymph nodes rather than the primary tumor, these clinical features are nearly compatible with previously reported features (14). Patients harboring one or more of these predictive factors may therefore derive the most benefit from *ALK* fusion gene screening.

Recently, *ALK*-positive NSCLC was reported to be a signet ring cell type adenocarcinoma (15, 16). We assume that this description also includes mucin production, i.e., mucin-producing tumors or tumors with >10% Alcian blue staining in the cytoplasm. Herein, we performed Alcian blue staining on suspected mucin-producing tumors as part of the histologic diagnosis. By this classification, 17 (15.6%) NSCLC cases were determined to be mucin-producing cancers. These cases were all adenocarcinomas and included five *ALK*-positive cases; thus, approximately 30% of the mucin-producing adenocarcinomas showed *ALK* positivity. This is a significantly high frequency compared with that of other NSCLCs ($P < 0.01$). This histologic feature, which can be assessed in cytologic samples, therefore seems to be useful for the prediction of *ALK* positivity.

The standard therapy for patients with advanced lung cancer at the time of presentation is chemotherapy and/or radiotherapy. However, standard platinum-based combined chemotherapy is not sufficient for disease eradication (17). Recently, lung cancer treatment strategies have become refined through the development of molecular markers and molecularly targeted agents. *ALK* inhibitors

have a high potential to become a definitive treatment for *ALK*-positive lung cancer, in a manner parallel to the exceptional therapeutic response of *EGFR*-positive lung cancers to *EGFR* tyrosine kinase inhibitors (18, 19). The efficacy of *ALK* inhibitors has been confirmed in cell lines (20, 21), and phase I clinical development of an oral *ALK* inhibitor for patients with lung cancer is currently under way (PF-02341066); two of the seven *ALK*-positive NSCLC cases from the present series have been enrolled in this trial (22, 23). As the background of *ALK*-positive lung cancer is similar to that of *EGFR*-positive lung cancer, and *ALK* tyrosine kinase inhibition is fundamentally similar to *EGFR* tyrosine kinase inhibition, *ALK* inhibitors might experience a similar progression of drug development and clinical and pathologic prediction of *ALK* positivity in lung cancer patients as *EGFR* tyrosine kinase inhibitors have for patients with *EGFR*-positive lung cancer. In this study, all *ALK*-positive lung cancers possessed wild-type *EGFR* and were therefore ineligible for *EGFR* tyrosine kinase inhibitor therapy (24). Therefore, *ALK* fusion gene assessment and administration of *ALK* inhibitors may become important for patients with *EGFR*-negative lung cancers.

Although some *ALK* inhibitors have already been developed and are currently being evaluated in clinical trials, it is important to establish a method for determining the existence of *ALK* fusion genes prior to the administration of *ALK* inhibitors. Both the presence of *ALK* fusion genes as well as *EGFR* gene mutations were successfully evaluated using histologic samples obtained by EBUS-TBNA of lung cancer regional lymph nodes. This diagnostic strategy allowed both pretreatment staging and evaluation of critical molecular markers to be definitively determined in a less invasive manner. There are some publications related with the genomic difference between primary tumor and metastatic site (25–29). EBUS-TBNA is a minimally invasive modality that allows the sampling of tumor cells from metastatic lymph node with a very low morbidity. The possibility of genetic differences should be considered whenever the biomarker information is used for the selection of patients for molecular target therapies. EBUS-TBNA is an ideal approach in this aspect.

In conclusion, EBUS-TBNA sampling is feasible for *ALK* fusion gene assessment by immunohistochemistry, FISH, and RT-PCR, as well as for pathologic diagnosis. The development of a safe and highly precise modality that enables the acquisition of a sufficient amount of high-quality tissue without surgery will become increasingly important in the molecularly targeted therapy era. EBUS-TBNA is one of the best candidates for such a methodology.

Disclosure of Potential Conflicts of Interest

K. Yasufuku, recipient of an unrestricted grant from Olympus Medical Corporation for Continuing Medical Education; H. Mano, member of the scientific advisory board, Pfizer Inc.

Acknowledgments

We thank Yuko Noguchi and Tetsushi Hirata for technical assistance with immunohistochemistry. We thank Drs. Yukiko Matsui, Masato Shingyoji, and Meiji Itakura for clinical analysis support. All authors have read and approved the final version of this manuscript.

Grant Support

This research was supported, in part, by the Ministry of Education, Culture, Sports, Science and Technology, Grant-in-Aid for Young Scientists (B) no. 21791340 in 2009 (T. Nakajima) and Grant-in-Aid for Cancer Research from Ministry of Health, Labor and Welfare in 2009 (T. Nakajima).

The costs of publication of this article were defrayed in part by the payment of page charges. This article must therefore be hereby marked *advertisement* in accordance with 18 U.S.C. Section 1734 solely to indicate this fact.

Received 01/14/2010; revised 06/14/2010; accepted 07/11/2010; published OnlineFirst 10/05/2010.

References

1. Mano H. Non-solid oncogenes in solid tumors: EML4-ALK fusion genes in lung cancer. Cancer Sci 2008;99:2349–55.
2. Soda M, Choi YL, Enomoto M, et al. Identification of the transforming EML4-ALK fusion gene in non-small-cell lung cancer. Nature 2007; 448:561–6.
3. Martelli MP, Sozzi G, Hernandez L, et al. EML4-ALK rearrangement in non-small cell lung cancer and non-tumor lung tissues. Am J Pathol 2009;174:661–70.
4. Takeuchi K, Choi YL, Togashi Y, et al. KIF5B-ALK, a novel fusion oncokinase identified by an immunohistochemistry-based diagnostic system for ALK-positive lung cancer. Clin Cancer Res 2009;15: 3143–9.
5. Nakajima T, Yasufuku K, Suzuki M, et al. Assessment of epidermal growth factor receptor mutation by endobronchial ultrasound-guided transbronchial needle aspiration. Chest 2007;132:597–602.
6. Yasufuku K, Chiyo M, Koh E, et al. Endobronchial ultrasound guided transbronchial needle aspiration for staging of lung cancer. Lung Cancer 2005;50:347–54.
7. Takeuchi K, Choi YL, Soda M, et al. Multiplex reverse transcription-PCR screening for EML4-ALK fusion transcripts. Clin Cancer Res 2008;14:6618–24.
8. Nagai Y, Miyazawa H, Huqun, et al. Genetic heterogeneity of the epidermal growth factor receptor in non-small cell lung cancer cell lines revealed by a rapid and sensitive detection system, the peptide nucleic acid-locked nucleic acid PCR clamp. Cancer Res 2005;65: 7276–82.
9. Yasufuku K, Chiyo M, Sekine Y, et al. Real-time endobronchial ultrasound-guided transbronchial needle aspiration of mediastinal and hilar lymph nodes. Chest 2004;126:122–8.
10. Herth FJ, Ernst A, Eberhardt R, Vilmann P, Dienemann H, Krasnik M. Endobronchial ultrasound-guided transbronchial needle aspiration of lymph nodes in the radiologically normal mediastinum. Eur Respir J 2006;28:910–4.
11. Herth FJ, Eberhardt R, Vilmann P, Krasnik M, Ernst A. Real-time endobronchial ultrasound guided transbronchial needle aspiration for sampling mediastinal lymph nodes. Thorax 2006;61:795–8.
12. Mino-Kenudson M, Chirieac LR, Law K, et al. A novel, highly sensitive antibody allows for the routine detection of ALK-rearranged lung adenocarcinomas by standard immunohistochemistry. Clin Cancer Res 2010;16:1561–71.
13. National Cancer Center Cancer Information Service. Available from: http://ganjoho.ncc.go.jp/public/statistics/backnumber/odjrh3000000vdf1-att/date02.pdf. Accessed on August 28, 2009.
14. Takahashi T, Sonobe M, Kobayashi M, et al. Clinicopathologic features of non-small-cell lung cancer with EML4-ALK fusion gene. Ann Surg Oncol 2010;17:889–97.

15. Inamura K, Takeuchi K, Togashi Y, et al. EML4-ALK fusion is linked to histological characteristics in a subset of lung cancers. J Thorac Oncol 2008;3:13–7.
16. Inamura K, Takeuchi K, Togashi Y, et al. EML4-ALK lung cancers are characterized by rare other mutations, a TTF-1 cell lineage, an acinar histology, and young onset. Mod Pathol 2009;22:508–15.
17. Wakelee H, Belani CP. Optimizing first-line treatment options for patients with advanced NSCLC. Oncologist 2005;10:1–10.
18. Lynch TJ, Bell DW, Sordella R, et al. Activating mutations in the epidermal growth factor receptor underlying responsiveness of non-small-cell lung cancer to gefitinib. N Engl J Med 2004;350: 2129–39.
19. Paez JG, Jänne PA, Lee JC, et al. EGFR mutations in lung cancer: correlation with clinical response to gefitinib therapy. Science 2004; 304:1497–500.
20. Koivunen JP, Mermel C, Zejnullahu K, et al. EML4-ALK fusion gene and efficacy of an ALK kinase inhibitor in lung cancer. Clin Cancer Res 2008;14:4275–83.
21. Piva R, Chiarle R, Manazza AD, et al. Ablation of oncogenic ALK is a viable therapeutic approach for anaplastic large-cell lymphomas. Blood 2006;107:689–97.
22. Kwak EL, Camidge DR, Clark J, et al. Clinical activity observed in a phase I dose escalation trial of an oral c-met and ALK inhibitor, PF-02341066. J Clin Oncol 2009;27:15s.
23. Christensen JG, Zou HY, Arango ME, et al. Cytoreductive antitumor activity of PF-2341066, a novel inhibitor of anaplastic lymphoma kinase and c-Met, in experimental models of anaplastic large-cell lymphoma. Mol Cancer Ther 2007;6:3314–22.
24. Shaw AT, Yeap BY, Mino-Kenudson M, et al. Clinical features and outcome of patients with non-small-cell lung cancer who harbor EML4-ALK. J Clin Oncol 2009;27:4247–53.
25. Kalikaki A, Koutsopoulos A, Trypaki M, et al. Comparison of EGFR and K-RAS gene status between primary tumours and corresponding metastases in NSCLC. Br J Cancer 2008;99:923–9.
26. Gow CH, Chang YL, Hsu YC, et al. Comparison of epidermal growth factor receptor mutations between primary and corresponding metastatic tumors in tyrosine kinase inhibitor-naive non-small-cell lung cancer. Ann Oncol 2009;20:696–702.
27. Daniele L, Cassoni P, Bacillo E, et al. Epidermal growth factor receptor gene in primary tumor and metastatic sites from non-small cell lung cancer. J Thorac Oncol 2009;4:684–8.
28. Park S, Holmes-Tisch AJ, Cho EY, et al. Discordance of molecular biomarkers associated with epidermal growth factor receptor pathway between primary tumors and lymph node metastasis in non-small cell lung cancer. J Thorac Oncol 2009;4:809–15.
29. Schmid K, Oehl N, Wrba F, et al. EGFR/KRAS/BRAF mutations in primary lung adenocarcinomas and corresponding locoregional lymph node metastases. Clin Cancer Res 2009;15:4554–60.

Lymphomatoid gastropathy: a distinct clinicopathologic entity of self-limited pseudomalignant NK-cell proliferation

Kengo Takeuchi,[1,2] Masahiro Yokoyama,[3] Shin Ishizawa,[4] Yasuhito Terui,[3] Kimie Nomura,[2] Kousuke Marutsuka,[5] Maki Nunomura,[6] Noriyasu Fukushima,[7] Takahiro Yagyuu,[8] Hirokazu Nakamine,[9] Futoshi Akiyama,[2] Kazuei Hoshi,[10] Kosei Matsue,[11] Kiyohiko Hatake,[3] and Kazuo Oshimi[12]

[1]Pathology Project for Molecular Targets and [2]Division of Pathology, The Cancer Institute, Japanese Foundation for Cancer Research, Tokyo, Japan; [3]Division of Hematology, The Cancer Institute Hospital, Japanese Foundation for Cancer Research, Tokyo, Japan; [4]Department of Pathology, Faculty of Medicine, University of Toyama, Toyama, Japan; [5]Pathology Division, Miyazaki Medical College Hospital, University of Miyazaki, Miyazaki, Japan; [6]Department of Pathology, Tachikawa Sougo Hospital, Tokyo, Japan; [7]Department of Internal Medicine, Faculty of Medicine, Saga University, Saga, Japan; [8]Department of Diagnostic Pathology, School of Medicine, Nara Medical University, Nara, Japan; [9]Department of Immunopathology, Kansai University of Health Sciences, Nara, Japan; [10]Department of Pathology, Kameda General Hospital, Chiba, Japan; [11]Division of Hematology/Oncology, Department of Medicine, Kameda General Hospital, Chiba, Japan; and [12]Eisai Research Institute of Boston, Andover, MA

Diagnostic errors in distinguishing between malignant and reactive processes can cause serious clinical consequences. We report 10 cases of unrecognized self-limited natural killer–cell proliferation in the stomach, designated as lymphomatoid gastropathy (LyGa). This study included 5 men and 5 women (age, 46-75 years) without any gastric symptoms. Gastroscopy showed elevated lesion(s) (diameter, ~ 1 cm). Histologically, medium-sized to large atypical cells diffusely infiltrated the lamina propria and, occasionally, the glandular epithelium. The cells were CD2$^{+/-}$, sCD3^{-}, cCD3^{+}, CD4^{-}, CD5^{-}, CD7^{+}, CD8^{-}, CD16^{-}, CD20^{-}, CD45^{+}, CD56^{+}, CD117^{-}, CD158a^{-}, CD161^{-}, T cell–restricted intracellular antigen-1^{+}, granzyme B^{+}, perforin^{+}, Epstein-Barr early RNA^{-}, T-cell receptor $\alpha\beta^{-}$, and T-cell receptor $\gamma\delta^{-}$. Analysis of the 16 specimens biopsied from 10 patients led to a diagnosis of lymphoma or suspected lymphoma in 11 specimens, gastritis for 1 specimen, adenocarcinoma for 1 specimen, and LyGa or suspected LyGa for 3 specimens. Most lesions underwent self-regression. Three cases relapsed, but none of the patients died. According to conventional histopathologic criteria, LyGa is probably diagnosed as lymphoma, especially as extranodal natural killer/T-cell lymphoma, nasal type. However, LyGa is recognized as a pseudomalignant process because of its clinical characteristics. The concept of LyGa should be well recognized. (*Blood.* 2010;116(25):5631-5637)

Introduction

The World Health Organization classification of tumors of hematopoietic and lymphoid tissues lists > 60 types of lymphomas.[1] Several reactive or borderline lesions related to these overt lymphomas are well known. Some benign lymphoproliferative disorders, including infectious mononucleosis, drug-induced lymphadenitis especially related to anticonvulsants, and histiocytic/subacute necrotizing lymphadenitis (Kikuchi-Fujimoto disease),[2,3] are occasionally misdiagnosed as malignancy because these lesions histopathologically mimic lymphoma.[4] They are basically self-limited and require no cytoreductive therapies. Lymphomatoid papulosis, lymphomatoid granulomatosis, and methotrexate-associated lymphoproliferative disorder[5] are listed as borderline lesions with uncertain malignant potential according to the World Health Organization. These disorders may also be diagnosed as overt lymphoma. Moreover, even if they are properly diagnosed, selection of a treatment strategy is then a matter of discussion because some of these cases undergo spontaneous regression. Therefore, conservative therapies are primarily favored in such cases, and these lesions should be treated as lymphoma only if they are clinically malignant. In any case, at the time these lesions are evaluated with biopsy specimens, the possibility of being benign should be well considered, and overtreatment must be carefully avoided.

Here, we report 10 cases of a pseudomalignant disorder caused by an unrecognized atypical natural killer (NK)–cell proliferation in the stomach; we have designated this disorder as lymphomatoid gastropathy (LyGa). According to conventional histopathologic criteria, such lesions are diagnosed as lymphoma, especially as extranodal NK/T-cell lymphoma, nasal type. However, considering its clinical characteristics, LyGa is recognized as a pseudomalignant process because it spontaneously regresses without any treatment.

Methods

Patients

During the 11-year period between 1998 and 2009, there were 10 cases of CD56-positive atypical lymphoid cell proliferation in the stomach (patients 1-3 presented at the Cancer Institute and patients 4-10 were referred to K.T. for consultation). The clinical records and pathology materials of the cases were reviewed.

Submitted June 15, 2010; accepted August 31, 2010. Prepublished online as *Blood* First Edition paper, September 9, 2010; DOI 10.1182/blood-2010-06-290650.

The publication costs of this article were defrayed in part by page charge payment. Therefore, and solely to indicate this fact, this article is hereby marked "advertisement" in accordance with 18 USC section 1734.

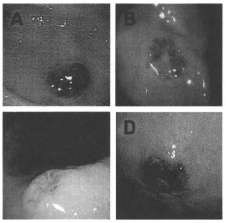

Figure 1. Gross appearance of LyGa. Cases 3 (A), 3 (B), 4 (C), and 10 (D) are shown.

Immunophenotyping and Epstein-Barr virus detection

Immunohistochemical examination was performed with Autostainer (Dako); dextran-polymer method (EnVision+; Dako); and antibodies against CD2, CD3, CD4, CD5, CD7, CD8, CD20, CD30, CD45, CD56, CD68 (KP1 or PGM1), T cell–restricted intracellular antigen-1 (TIA1), granzyme B, anaplastic lymphoma kinase, myeloperoxidase, Ki67, and T-cell receptor βF1 (TCRβF1). For flow cytometry, the following antibodies were used: CD2, CD3, CD7, CD56, TCRαβ, TCRγδ, TCRVa24, CD158a, and CD161. The presence of Epstein-Barr virus (EBV) was assessed by in situ hybridization for Epstein-Barr early RNA (EBER).

Polymerase chain reaction analysis for TCRγ gene rearrangement

DNA was extracted from the paraffin sections with the use of Recover All Total Nucleic Acid Isolation according to the manufacturer's instructions (Ambion). A seminested protocol involving 2 rounds of polymerase chain reaction (PCR) was used for the amplification of the rearranged TCRγ gene with the use of the primers TVγ, 5′-AGGGTTGTGTTGGAATCAGG-3′; TJγ-out, 5′-CGTCGACAACAAGTGTTGTTCCAC-3′; and TJγ-in, 5′-GGATCCACTGCCAAAGAGTTTCTT-3′. The 5′ end of TJγ-I was labeled by cyanine 5 for fragment analysis. In all the experiments, monoclonal (Jurkat cells) and polyclonal (placental tissue from a healthy person) controls were run in parallel with the samples. The PCR products were analyzed with CEQ8000 (Beckman Coulter Inc). DNA from each sample was amplified ≥ 6 times.

Results

Clinical history

Of the 10 patients in this study, 5 were men and 5 were women. The age of these patients ranged from 46 to 75 years Three patients had a history of gastric cancer, of whom 1 had previously undergone endoscopic mucosal resection 2 times (case 1) and the other 2 had previously undergone partial gastrectomy (cases 3 and 8). At the time of the study, 3 patients had diabetes mellitus (cases 1, 2, and 9) and 4 had hypertension (cases 2, 7, 9, and 10). Blood cell counts and chemistry, including lactic dehydrogenase levels, were within the normal limits in all patients. There were no gastric symptoms at the time of gastroscopy. The 3 patients with history of gastric cancer underwent gastroscopy during a follow-up study for gastric cancer, and the procedure was performed on the other patients as a secondary checkup because gastric x-ray screening for cancer in these patients showed the presence of abnormal shadows. Gastroscopy showed ulcerative or elevated lesion(s) ~ 1 cm in diameter in the stomach (Figure 1A-D). The pathologists of the institutions where the biopsies of the patients with LyGa were first performed diagnosed the patients' conditions as lymphoma or suspected lymphoma (cases 1, 2, 5-8, and 10), gastritis with histiocytic infiltration (case 3), and poorly differentiated adenocarcinoma (case 4). In case 3, the specimen was biopsied again 11 months later, and the patient's condition was then diagnosed as NK/T-cell lymphoma. Cases 5 and 9 were suspected of having lymphoma, and the pathologist consulted with one of the authors (K.T.), leading to the diagnosis of LyGa. In case 5, another biopsy was performed 3 weeks after the first biopsy for flow cytometry.

An extensive workup, including ultrasonography (cases 1-4 and 9), computed tomographic (cases 1-4 and 6-9), and 2-[fluorine-18]fluoro-2-deoxy-D-glucose positron emission tomographic scans (cases 2, 4, 6, and 8); colonoscopy (cases 2, 4-6, and 9); and bone marrow biopsy (cases 1-4 and 7-9), was performed. The results showed no evidence of lymphoma in sites other than the stomach. Multiple serologic studies for celiac disease showed no evidence of high titers of anti–gliadin immunoglobulin A and immunoglobulin G antibodies in cases 2 and 4. Gastroscopy and biopsy were performed 1-4 months after the biopsies, which showed no evidence of lymphoma (cases 1, 2, 5, 7 and 10). Cases 4 and 6 underwent partial gastrectomy 1 month after the initial biopsy diagnosis, resulting in no evidence of carcinoma or lymphoma. All the patients were carefully watched and followed up without chemotherapy. Except in the case of patients 3, 8, and 9, none of the other patients had any recurrences. In case 3, the patient developed 3 lesions; on follow-up examination 11 months later, the lesions had regressed, and a new lesion was detected. The new lesion also regressed in 1 month from the second biopsy. In case 8, the patient developed another lesion 7 months after self-regression of the first lesion; this new lesion also regressed in 3 months without any treatment. In case 9, the first lesion could not be detected 4 months from the first biopsy; however, 2 new lesions were detected. After another 4 months, these 2 lesions could also not be detected, and 2 new lesions were identified. The consequence of the 2 lesions last detected is unknown because the patient refused further gastroscopic examination.

Morphology

Grossly, the lesions were flat elevations with or without a shallow depression and were approximately 1 cm in diameter (Figure 1A-D). The atypical cells diffusely infiltrated the lamina propria and occasionally into the glandular epithelium (Figure 2A), simulating the lymphoepithelial lesion seen in extranodal marginal zone lymphoma of mucosa-associated lymphoid tissue lymphoma, which was designated as lymphoepithelial-like lesion by NK cells (Figure 2B). In some cases, necrosis was present, but there were no angiocentric or angiodestructive growth patterns or apoptotic bodies. Mitotic figures were occasionally present. The atypical cells were medium to large with moderate to abundant clear or slightly eosinophilic cytoplasm. The nuclei were generally round to oval, but some were irregular and indented, with fine chromatin and a few inconspicuous nucleoli. These cytomorphologic features somewhat give a histiocyte-like impression. Interestingly, specimens for all the patients contained a variable proportion of cells (20%-90%) with eosinophilic granules in the cytoplasm (Figure 2C-D). In some cases, atypical cells with a prominent nucleolus were observed (Figure 2D). Small reactive lymphocyte aggregates and neutrophils may be occasionally found. Nine of the patients had *Helicobacter pylori* infection.

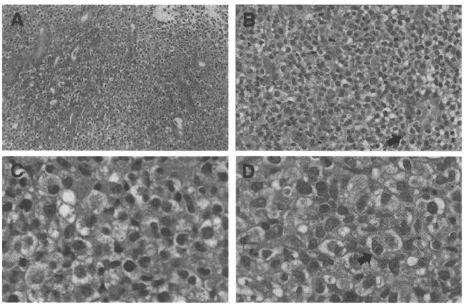

Figure 2. Histopathology of LyGa. The pattern of infiltration is diffuse (A; case 1; 20× objective). Atypical NK cells occasionally infiltrate the glandular epithelium (arrow), showing lymphoepithelial-like lesions by NK cells (B; case 10; 40× objective). Some atypical cells harbor large eosinophilic granules in the cytoplasm (C; case 3; 100× objective). In some cases, the nucleoli are prominent (arrow; D; case 5; 100× objective). Figures were taken with a microscope (BX51; Olympus) and a digital camera (KY-F75; Victor). Microsoft PowerPoint 2007 was used for image processing. Numeric apertures: 20×/0.40 (A), 40×/0.75 (B), 40×/0.95 (C), 60×/0.90 (D).

Immunophenotype and EBER in situ hybridization

The atypical cells were strongly positive for CD7, CD56, and cytotoxic molecule-associated proteins (TIA1, granzyme B, and perforin; Figure 3A-C). CD2 and CD45 were variably positive. CD3ε was positive in the cytoplasm, but a membrane-staining pattern was not observed (Figure 3D). Anaplastic large cell lymphoma-associated markers (CD30 and anaplastic lymphoma kinase) were negative. Other common lineage markers, including B-cell (CD20), T-cell (CD4, CD5, and CD8), and myelomonocytic (CD68 and myeloperoxidase) markers, were all negative. EBER in situ hybridization was negative. The results of immunohistochemistry for individual cases are listed in Table 1. For case 5, flow cytometric analysis was performed with the second specimen, which was obtained from a biopsy performed 3 weeks after the first biopsy (Figure 4). Grossly, although the lesion was regressing, it remained present. The atypical cells of this case expressed CD7 and CD56 (both aberrantly bright) and CD2 (negative or dim). Other T or NK cell–related markers were negative (CD3, CD16, TCRαβ, TCRγδ, TCRVa24, CD158a, and CD161).

PCR analysis for TCRγ gene rearrangement

PCR analysis for TCRγ gene rearrangement was performed 6 times per case for cases 1-4 and 8. No reproducible rearranged bands were observed (data not shown).

Discussion

Here, we report 10 cases of self-limited lymphoma-like lesions in the stomach, which we designated as LyGa. These cases were almost identical to each other in morphology and immunophenotype of atypical cells. Gross examination showed that the lesions were ulcers or flat elevations with a shallow depression, measuring approximately 1 cm in diameter. Microscopic observation showed that they were composed of sheets of large peculiar cells that showed indented nuclei and clear cytoplasm with eosinophilic granules. Immunohistochemical analysis of the atypical cells of LyGa showed that they were $CD2^-$ or variably $CD2^+$, $CD3^+$ (cytoplasmic), $CD4^-$, $CD5^-$, $CD7^+$, $CD8^-$, $CD16^-$, $CD20^-$,

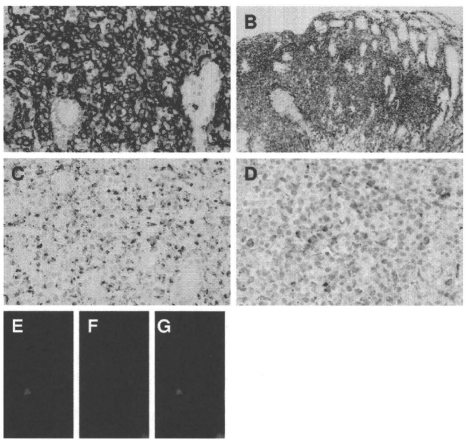

Figure 3. Immunophenotype of LyGa by immunohistochemistry. The atypical cells are positive for CD7 (A; case 5), CD56 (B; case 3), granzyme B (C; case 4), and cytoplasmic CD3ε (D; case 2). To confirm the cytoplasmic localization of CD3ε, fluorescein double immunohistochemistry for CD3ε (E) and CD56 (F) was performed (case 10). In the merged figure (G), the cytoplasmic localization of CD3ε is clearly shown, indicating that the atypical cells are of NK lineage. Figures were taken with a microscope (BX51; Olympus) and a digital camera (KY-F75; Victor). Microsoft PowerPoint 2007 was used for image processing. Numeric apertures: 40× (A,C,D), 10× (B), 60× (E-G).

Table 1. Patient characteristics and immunologic markers

	Case 1	Case 2	Case 3	Case 4	Case 5	Case 6	Case 7	Case 8	Case 9	Case 10
Age, y	52	58	51	50	55	46	65	56	59	75
Sex	Male	Male	Male	Female	Male	Male	Female	Female	Female	Female
Past history	Two individual early gastric cancers at the ages of 48 and 51 y	NP	Advanced gastric cancer at the age of 47 y	NP	NP	NP	NP	Advanced gastric cancer at the age of 52	NP	NP
H pylori	–	+	+	+	+	+	+	+	+	+
Original pathologic diagnosis	NK/T-cell lymphoma	NK/T-cell lymphoma	Gastritis with histiocytosis. NK/T-cell lymphoma*	Adenocarcinoma	Lymphoma, s/o LyGa*	NK/T-cell lymphoma; NK/T-cell lymphoma*	T-cell lymphoma	T-cell lymphoma; NK/T-cell lymphoma*	Lymphoma, s/o LyGa, s/o LyGa*	T-cell lymphoma
Follow-up examinations, days from the initial biopsy	45, 73, 276, 577, 1165	55, 239, 442, 675, 896, 1121, 1497	336,† 365, 484, 701, 1065, 1429, 1793	41,‡ 167, 1360	13,† 132	50,† 56‡	38, 81, 137, 207, 361, 515, 742, 1029, 1281, 1515	98, 154, 236,† 256, 333, 452, 585, 790	113,† 232†	30, 59, 143, 232, 354
Patient status	Well at 145 mo	Well at 50 mo	Well at 60 mo	Well at 46 mo	Well at 33 mo	Well at 60 mo	Well at 56 mo	Well at 29 mo	Well at 18 mo	Well at 12 mo
Treatment	Observation	Observation	Observation	Subtotal gastrectomy	Observation	Total gastrectomy	Observation	Observation	Observation	Observation
CD2	–	+w	+w	+w	–	+	+w	–	+	+
CD3	+	+	+	+	+	+	+	+	+	+
CD4	ND	–	–	–	–	–	–	–	–	–
CD5	–	–	–	–	–	–	–	–	–	–
CD7	+	+	+	+	+	+	+	+	+	+
CD8	ND	–	–	ND	–	–	–	–	–	–
CD20	–	–	–	–	–	–	–	–	–	–
CD56	+	+	+	+	+	+	+	+	+	+
Cytotoxic molecules	TIA1$^+$	TIA1$^+$, granzyme B$^+$, perforin$^+$	TIA1$^+$, granzyme B$^+$, perforin$^+$	TIA1$^+$, granzyme B$^+$, perforin$^+$	Granzyme B$^+$	TIA1$^+$, Perforin$^+$	Perforin$^+$	TIA1$^+$	Granzyme B$^+$	Granzyme B$^+$
EBER	–	–	–	–	–	–	–	–	–	–
Other markers	CD16$^-$, betaF1$^-$	CD16$^-$, CD30$^-$, CD45$^+$w, CD57$^-$, CD68$^-$, CD123$^-$, betaF1$^-$, ALK$^-$, MPO$^-$, MIB1 index 10%	CD16$^-$, CD30$^-$, CD45$^+$w, CD57$^-$, CD68$^-$, CD123$^-$, betaF1$^-$, ALK$^-$, TdT$^-$, MIB1 index 30%	CD16$^-$, CD45$^+$, CD68$^-$, CD123$^-$, betaF1$^-$, CD43$^+$	TCRαβ$^-$, TCRγδ$^-$, CD161$^-$, TCRVα24$^-$, CD16$^-$, CD158a$^-$				CD10$^-$, CD21$^-$, BCL2$^+$, CD45RO$^+$, CD68$^-$, MIB1 index 20%	MIB1 index 20%, CD21$^-$

NP indicates nothing in particular; s/o, suspected of; ND, not done; and +w, weakly positive.

*In case 3, 5, 6, 8 and 9, multiple biopsies showed the presence of LyGa.

†LyGa is present on follow-up examination.

‡In follow-up examinations, days of gastrectomy or gastroscopy with or without biopsy from the initial biopsy are described.

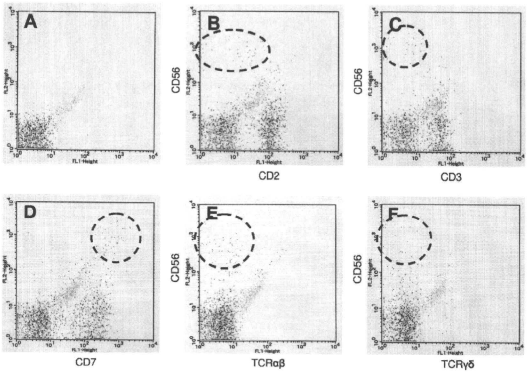

Figure 4. Immunophenotype of LyGa by flow cytometry. Flow cytometry was performed for case 5. The atypical cells were $CD56^{bright}$, $CD2^{dim}$ (B), $CD3^-$ (C), $CD7^{bright}$ (D), $TCR\alpha\beta^-$ (E), and $TCR\gamma\delta^-$ (F). (A) Negative control.

$CD45^+$, $CD56^+$, $CD117^-$ and positive for cytotoxic molecule-related proteins ($TIA1^+$, granzyme B^+, and perforin$^+$). This immunophenotype is highly suggestive of extranodal NK/T-cell lymphoma of the nasal type, which usually arises in extranodal sites, especially in the nasal cavity.[1,6,7]

Extranodal NK/T-cell lymphoma of the nasal type is rarely seen in Western countries and is more common in Asia and in Central and South American countries.[1,6,7] It accounts for ~ 2%,[8] 6%,[9] 8%,[10] and 5%[11] of all newly diagnosed lymphoma cases in Japan, Hong Kong, Korea, and Taiwan, respectively. Histologically, the lymphoma often has an angiocentric and angiodestructive infiltrate of atypical lymphocytes of various sizes leading to extensive necrosis.[1] The immunophenotype of neoplastic cells usually indicates that they are of NK-cell lineage (surface $CD3^-$, cytoplasmic $CD3^+$, $CD5^-$, and $CD56^+$) but are occasionally of T-cell lineage by definition.[1] In previous studies, neoplastic cells in almost all the cases were found to be infected by EBV.[12,13] In localized diseases, the survival rate has recently improved with a combination of upfront radiotherapy and chemotherapy, whereas almost all patients with extensive disease die within a year after diagnosis.[14-16]

Of the 16 biopsied specimens in this study, 11 were diagnosed with lymphoma or suspected lymphoma. Fortunately, however, LyGa has several characteristic features that are not consistent with extranodal NK/T-cell lymphoma. First, the stomach is not a common site of origin in the case of NK/T-cell lymphoma. To the best of our knowledge, there are 10 reported cases of extranodal NK/T-cell lymphoma involving the stomach, and the lesions were not limited to the stomach in any of these cases.[17-21] Second, although some of the cases of LyGa showed necrosis, but angiocentric or angiodestructive growth patterns, and prominent apoptotic bodies, which are common features of extranodal NK/T-cell lymphoma,[1] were not observed. Third, LyGa may show epithelial invasion, that is, lymphoepithelial-like lesion by NK cells. Fourth, the cytomorphology of LyGa is atypical for extranodal NK/T-cell lymphoma. Although the cytologic spectrum of extranodal NK/T-cell lymphoma is broad,[1] to the best of our knowledge, large eosinophilic cytoplasmic granules seen in the atypical cells of LyGa have never been observed in the histopathology section of extranodal NK/T-cell lymphoma although finer granules can often be seen in Giemsa-stained cytologic preparations. Finally, EBER in situ hybridization, which is almost always positive in NK/T-cell lymphoma of the nasal type,[1,12,13] is consistently negative in LyGa. In addition, a differential diagnosis of $CD56^+$ T-cell neoplasm with extensive loss of T-cell markers may be considered. In particular, the immunophenotype of LyGa overlaps the immunophenotype observed in some cases of enteropathy-associated T-cell lymphoma (type II).[22] However, the negative PCR results for the TCRγ gene rearrangement (performed in cases 1-4 and 8; data not shown) were inconsistent with results obtained for T-cell lymphomas.

Vega et al[23] reported a similar case of atypical NK-cell proliferation probably related to gluten sensitivity mimicking NK-cell lymphoma. In that study, the 32-year-old male patient was positive for anti–gliadin antibody and had persistent multiple lesions in the stomach, small bowel, and large bowel for 3 years.[23] Two of our 10 patients were tested and found to be negative for anti–gliadin antibodies. Actually, gluten intolerance and celiac disease are extremely rare in Japan. However, the immunophenotype and morphology of the atypical cells of our patients were similar to those observed in the case of the 32-year-old man reported by Vega et al.[23] In addition, our cases shared a significant clinical feature with the case reported by Vega et al,[23] that is, "self regression." The lesions of the 32-year-old man persisted for 3 years until he was placed on a gluten- and lactose-free diet, whereas the lesions of our patients did not seem to persist for such an extended period of time. Furthermore, none of our patients were found to have intestinal lesions. These differences might be due to the different stimulants, if any, although we were unable to identify any stimulant(s) in our cases.

Two types of gastric malignant neoplasms, namely, adenocarcinoma and mucosa-associated lymphoid tissue lymphoma, are related to *H pylori* infection. Nine of the 10 cases were positive for *H pylori* infection, and 3 of the patients had a history of gastric adenocarcinoma. Normal NK cells were present in both *H pylori*–infected and uninfected gastric mucosa at approximately 6% and 15% of the infiltrating lymphocytes, respectively.[24] Several of our patients received *H pylori* eradication therapy, and their LyGa was observed to regress. There may be a pathogenetic relationship between *H pylori* and LyGa. However, ~ 82% of the Japanese population is infected with *H pylori*.[25] Moreover, even patients who did not undergo eradication therapy exhibited regression of LyGa. In terms of the relation of LyGa with adenocarcinoma, LyGa is more likely to be found in persons who have frequently

undergone gastroscopy because LyGa shows no gastric symptoms. Therefore, although these concomitant occurrences appear coincidental, further studies are required for a better understanding of LyGa and its relationship with adenocarcinoma.

Whether LyGa is monoclonal proliferation or not remains a matter of debate. Unlike B or T cells, NK cells do not undergo any specific gene rearrangement, rendering it difficult to determine whether the proliferation of EBV-free NK cells is monoclonal or not. Vega et al[23] indicated that the NK-cell proliferation in their study appeared polyclonal because of the heterogeneous expression of the immunoglobulin-like receptors CD158a, CD158b, and CD158e; nevertheless, they could not exclude the possibility of a low-grade neoplasm. Siu et al[26] reported that the p73 gene was methylated in 94% of the NK-cell malignancies and that other methylated genes included *hMLH1* (63%), *p16* (63%), *p15* (48%), and *RAR* β (47%). We analyzed the methylation status of several genes, including *p16*, *p73*, *DAPK*, *MGMT*, *CDH1*, and *hMLH1*, in 2 heterochronically biopsied specimens from case 3 to obtain evidence of monoclonality. No aberrant methylation, however, was found in the examined genes (data not shown). These results reconfirmed that LyGa is different from extranodal NK/T-cell lymphoma, but the results did not serve as evidence for the monoclonality of LyGa. Further investigation with a larger sample size is required to clarify this distinction. Cytogenetic analyses and studies involving the identification of genetic loss/gain (eg, studies involving single nucleotide polymorphism microarray analysis) or point mutations (eg, studies involving next-generation genome sequencing) may be helpful to clarify the biologic natures of LyGa, especially whether LyGa is monoclonal proliferation or not. Procurement of fresh materials for these studies is impeded by spontaneous regression of lesions after the index biopsy; the biopsy specimen is usually fixed in formalin and embedded in paraffin for routine pathologic diagnosis.

LyGa should be regarded as a distinctive clinicopathologic entity and be observed without treatment. However, if not well recognized, LyGa is probably to be histopathologically misdiagnosed as lymphoma. For example, Kikuchi-Fujimoto disease, a self-limiting disorder of unknown cause, is still often mistakenly diagnosed as lymphoma,[4] although > 30 years have passed since it was first described in 1972. If LyGa is misdiagnosed as NK/T-cell lymphoma, it might be treated with radical therapeutic procedures, including chemotherapy, radiotherapy, gastrectomy, and stem cell transplantation. In fact, 2 patients of the present series underwent gastrectomy. The remaining 8 patients did not receive any treatment because the staging procedures followed by the initial diagnosis showed that the lesions regressed spontaneously. For 1 patient, however, the first biopsy specimen diagnosed as lymphoma was suspected to have been mistakenly identified to the patient. Fortunately, LyGa shows highly conserved and characteristic features in terms of clinical presentation, morphology, and immunophenotype (immunohistochemistry for CD3, CD5, CD7, CD56, and cytotoxic molecule(s) and EBER in situ hybridization are required to diagnose LyGa). Therefore, as long as LyGa is recognized as a distinct disease concept, there is no scope of misdiagnosis as malignancy.

Acknowledgments

We thank Drs Hiroshi Takahashi, Toshio Kumasaka, Yukiko Itoh, Satoko Hatano, Keiko Yoshimura, Kazuya Kobori, and Takanori Kuwabara and the members of Ganken Ariake Lymphoma Study Group (GALSG) for their advice.

This work was supported in part by Grants-in-Aid for Scientific Research from the Ministry of Education, Culture, Sports, Science, and Technology, Japan.

Authorship

Contribution: K.T. and K.O. conceived the study, collected and analyzed the data, and drafted the paper; M.Y., Y.T., K. Marutsuka, M.N., N.F., T.Y., H.N., F.A., K. Hoshi, K. Matsue, and K. Hatake contributed patient materials and analyzed the data; and S.I. and K.N. performed special studies and analyzed the data.

Conflict-of-interest disclosure: The authors declare no competing financial interests.

Correspondence: Kengo Takeuchi, Pathology Project for Molecular Targets, Cancer Institute, Japanese Foundation for Cancer Research, 3-8-31 Ariake, Koto, Tokyo 135-8550, Japan; e-mail: kentakeuchi-tky@umin.net.

References

1. Swerdlow SH, Campo E, Harris NL, et al, eds. *WHO Classification of Tumours of Haematopoietic and Lymphoid Tissues*. Lyon, France: IARC Press; 2008.
2. Kikuchi M. Lymphadenitis showing focal reticulum cell hyperplasia with nuclear debris and phagocytosis. *Nippon Ketsueki Gakkai Zasshi*. 1972;35:379-380.
3. Fujimoto Y, Kozima Y, Yamaguchi K. Cervical subacute necrotizing lymphadenitis: a new clinicopathologic entity. *Naika*. 1972;20:920-927.
4. Menasce LP, Banerjee SS, Edmondson D, Harris M. Histiocytic necrotizing lymphadenitis (Kikuchi-Fujimoto disease): continuing diagnostic difficulties. *Histopathology*. 1998;33(3):248-254.
5. Kamel OW, van de Rijn M, Weiss LM, et al. Brief report: reversible lymphomas associated with Epstein-Barr virus occurring during methotrexate therapy for rheumatoid arthritis and dermatomyositis. *N Engl J Med*. 1993;328(18):1317-1321.
6. Oshimi K. Progress in understanding and managing natural killer-cell malignancies. *Br J Haematol*. 2007;139(4):532-544.
7. Suzuki R, Takeuchi K, Ohshima K, Nakamura S. Extranodal NK/T-cell lymphoma: diagnosis and treatment cues. *Hematol Oncol*. 2008;26(2):66-72.
8. The World Health Organization classification of malignant lymphomas in Japan: incidence of recently recognized entities. Lymphoma Study Group of Japanese Pathologists. *Pathol Int*. 2000;50(9):696-702.
9. Au WY, Ma SY, Chim CS, et al. Clinicopathologic features and treatment outcome of mature T-cell and natural killer-cell lymphomas diagnosed according to the World Health Organization classification scheme: a single center experience of 10 years. *Ann Oncol*. 2005;16(2):206-214.
10. Ko YH, Kim CW, Park CS, et al. REAL classification of malignant lymphomas in the Republic of Korea: incidence of recently recognized entities and changes in clinicopathologic features. Hematolymphoreticular Study Group of the Korean Society of Pathologists. Revised European-American lymphoma. *Cancer*. 1998;83(4):806-812.
11. Chen CY, Yao M, Tang JL, et al. Chromosomal abnormalities of 200 Chinese patients with non-Hodgkin's lymphoma in Taiwan: with special reference to T-cell lymphoma. *Ann Oncol*. 2004;15(7):1091-1096.
12. Harabuchi Y, Yamanaka N, Kataura A, et al. Epstein-Barr virus in nasal T-cell lymphomas in patients with lethal midline granuloma. *Lancet*. 1990;335(8682):128-130.
13. Jaffe ES, Chan JK, Su IJ, et al. Report of the Workshop on Nasal and Related Extranodal Angiocentric T/Natural Killer Cell Lymphomas. Definitions, differential diagnosis, and epidemiology. *Am J Surg Pathol*. 1996;20(1):103-111.
14. Aviles A, Diaz NR, Neri N, Cleto S, Talavera A. Angiocentric nasal T/natural killer cell lymphoma: a single centre study of prognostic factors in 108 patients. *Clin Lab Haematol*. 2000;22(4):215-220.
15. Ribrag V, Ell Hajj M, Janot F, et al. Early locoregional high-dose radiotherapy is associated with long-term disease control in localized primary angiocentric lymphoma of the nose and nasopharynx. *Leukemia*. 2001;15(7):1123-1126.
16. Shikama N, Ikeda H, Nakamura S, et al. Localized aggressive non-Hodgkin's lymphoma of the nasal cavity: a survey by the Japan Lymphoma Radiation Therapy Group. *Int J Radiat Oncol Biol Phys*. 2001;51(5):1228-1233.
17. Zhang YC, Sha Z, Yu JB, et al. Gastric involvement of extranodal NK/T-cell lymphoma, nasal

type: a report of 3 cases with literature review. *Int J Surg Pathol.* 2008;16(4):450-454.

18. Kim JH, Lee JH, Lee J, et al. Primary NK-/T-cell lymphoma of the gastrointestinal tract: clinical characteristics and endoscopic findings. *Endoscopy.* 2007;39(2):156-160.
19. Ko YH, Cho EY, Kim JE, et al. NK and NK-like T-cell lymphoma in extranasal sites: a comparative clinicopathological study according to site and EBV status. *Histopathology.* 2004;44(5):480-489.
20. Sasaki M, Matsue K, Takeuchi M, Mitome M, Hirose Y. Successful treatment of disseminated nasal NK/T-cell lymphoma using double autologous peripheral blood stem cell transplantation. *Int J Hematol.* 2000;71(1):75-78.
21. Chan JK, Tsang WY, Lau WH, et al. Aggressive T/natural killer cell lymphoma presenting as testicular tumor. *Cancer.* 1996;77(6):1198-1205.
22. Zettl A, deLeeuw R, Haralambieva E, Mueller-Hermelink HK. Enteropathy-type T-cell lymphoma. *Am J Clin Pathol.* 2007;127(5): 701-706.
23. Vega F, Chang CC, Schwartz MR, et al. Atypical NK-cell proliferation of the gastrointestinal tract in a patient with antigliadin antibodies but not celiac disease. *Am J Surg Pathol.* 2006;30(4):539-544.
24. Yun CH, Lundgren A, Azem J, et al. Natural killer cells and Helicobacter pylori infection: bacterial antigens and interleukin-12 act synergistically to induce gamma interferon production. *Infect Immun.* 2005;73(3):1482-1490.
25. Uemura N, Okamoto S, Yamamoto S, et al. Helicobacter pylori infection and the development of gastric cancer. *N Engl J Med.* 2001;345(11): 784-789.
26. Siu LL, Chan JK, Wong KF, Kwong YL. Specific patterns of gene methylation in natural killer cell lymphomas: p73 is consistently involved. *Am J Pathol.* 2002;160(1):59-66.

Sorafenib-induced erythema multiforme for metastatic renal cell carcinoma

Sorafenib is an active agent for cytokine-refractory renal cell carcinoma (RCC) patients [1]. Skin toxicity such as hand–foot syndrome (HFS) is one of the frequent adverse events of sorafenib. In the phase II study conducted in Japan, grade 3 skin toxicity occurred in 13.7% of 131 patients with RCC, but all of those skin toxic effects were HFS or rash/desquamation [2]. We here report three cases of erythema multiforme (EM) associated with sorafenib therapy. EM, Stevens–Johnson syndrome, and toxic epidermal necrolysis are mucocutaneous diseases associated with significant morbidity and mortality. The term 'Stevens–Johnson syndrome' has been widely accepted as a synonym for EM major [3].

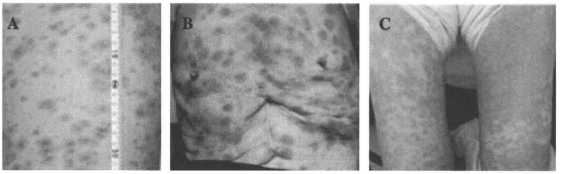

Figure 1. Erhythema multiforme of three cases. Target-like erythematous skin rash of left femoral lesion of case 1 (A), case 2 (B), and case 3 (C).

case 1

A 25-year-old female with pulmonary metastases of papillary RCC received sorafenib 800 mg/day. At day 8, erythema appeared on lower legs and spread over 50% of body surface area in 2 days (Figure 1A) with HFS. She also suffered intermittent fever up to 39.5°C from day 8. Serum examination excluded the viral infection, including measles, herpes simplex, or herpes zoster. Skin biopsy of femoral region at day 12 revealed superficial and perivascular lymphocyte infiltration and necrotic keratinocytes, compatible with EM. Skin rash disappeared within days after discontinuation of sorafenib without steroid treatment or antimicrobial treatment.

case 2

An 80-year-old man with multiple pulmonary metastases of papillary RCC was treated with sorafenib 800 mg/day. From the 8th to 12th day of sorafenib, erythema spread over his whole body (Figure 1B) with grade 2 HFS, mild stomatitis, and grade 3 fatigue. EM and HFS disappeared within 2 weeks after discontinuation of sorafenib and oral predonisolone 10 mg/day. When sorafenib (400 mg/day) was rechallenged, EM with high fever reappeared within 24 h and the sorafenib was discontinued at once.

case 3

A 70-year-old female with metastatic clear cell RCC developed erythema spread to whole body 15 days after starting sorafenib 800 mg/day (Figure 1C). Eruption disappeared within 2 weeks after discontinuation of sorafenib and topical treatment without steroid. She was treated with sunitinib 50 mg/day and EM has not appeared.

Rash, desquamation, and HFS are most frequent skin symptoms with sorafenib. They are dose dependent and disappear with discontinuation of sorafenib. In most cases, restart with the same dose is possible and the symptoms may resolve without dose modification. MacGregor et al. [4] reported sorafenib-induced EM in malignant melanoma patient. They carried out skin biopsy and showed the same findings with that of our case. In that report, the patient was rechallenged with the reduced dose of sorafenib (100 mg) but developed the same eruption within 24 h, and they discontinued sorafenib. There have been only two other reports about sorafenib-induced EM [5, 6], but we experienced three EM patients, one of which was confirmed by biopsy, of 16 RCC patients we have treated with sorafenib in a year.

Furthermore, postmarketing surveillance of sorafenib-treated patients in Japan reported that 108 cases of so-called EM occurred in 2889 cases from February 2008 to October 2009, so occurrence rate of EM might be different between Japanese and Caucasians. A recent study suggests that polymorphisms in specific genes encoding for metabolizing enzymes, efflux transporters, and drug targets are associated with toxic effects of sunitinib, another angiogenesis inhibitor [7]. In addition, the population-related pharmacogenomics might contribute to differences in adverse events and responses of antitumor agents between patients in Japan and those in the United States [8]. Further study is necessary to elucidate this discrepancy of EM occurrence rate between Japanese and Caucasians.

In clinical practice, it is very difficult to diagnose whether the drug-induced skin rash is caused by allergic or toxic mechanisms. To use sorafenib safely, restarting of sorafenib needs careful monitoring because the possibility of an allergic mechanism cannot be ruled out. Patients with skin lesions due to allergic mechanisms may not have benefits from sorafenib treatment because of early treatment failure. At present, we cannot recommend the rechallenge of sorafenifb for these patients as two of three patients including our case recurred EM.

Sorafenib is now one of few standard agents for metastatic RCC. Molecular mechanism of this type of toxicity remains unknown. Further investigation is necessary to disclose the mechanism and establish the effective therapy for sorafenib-induced EM, which might not be a rare adverse event in Japanese patients.

M. Kodaira[1], S. Takahashi[1]*, K. Takeuchi[2], T. Yuasa[1]
T. Saotome[1], J. Yonese[3], I. Fukui[3] & K. Hatake[1]

[1]Department of Medical Oncology, Cancer Institute Hospital of Japanese Foundation for Cancer Research, [2]Department of Pathology and [3]Department of Urology, Cancer Institute of Japanese Foundation for Cancer Research, Tokyo, Japan
(*E-mail: stakahas@jfcr.or.jp)

disclosure

None of the authors declare conflicts of interest.

references

1. Escudier B, Eisen T, Stadler WM et al. Sorafenib in advanced clear-cell renal cell carcinoma. N Eng J Med 2007; 356: 125–134.

2. Akaza H, Tsukamoto T, Murai M et al. Phase II study to investigate the efficacy, safety, and pharmacokinetics of sorafenib in Japanese patients with advanced renal cell carcinoma. Jpn J Clin Oncol 2007; 37: 755–762.
3. Roujeau JC, Stern RS. Severe adverse cutaneous reactions to drugs. N Engl J Med 1994; 331: 1272–1285.
4. MacGrecor JL, Silber DN, Grossman ME et al. Sorafenib induced erythema multiforme. J Am Acad Dermatol 2007; 56: 527–528.
5. Bilac C, Muezzinoglu T, Ermertcan AT et al. Sorafenib-induced erythema multiforme in metastatic renal cell carcinoma. Cutan Ocul Toxicol 2009; 28: 90–92.
6. Feltes RA, Feito Rodriguez M, Gonzalez-Beato MJ. Erythema multiforme induced by sorafenib. Clin Exp Dermatol 2009; 34: e368–e369.
7. Van Erp NP, Eechoute K, van der Veldt AA et al. Pharmacogenetic pathway analysis for determination of sunitinib-induced toxicity. J Clin Oncol 2009; 27: 4406–4412.
8. Gandara DR, Kawaguchi T, Crowley J et al. Japanese-US common-arm analysis of paclitaxel plus carboplatin in advanced non-small-cell lung cancer: a model for assessing population-related pharmacogenomics. J Clin Oncol 2009; 27: 3540–3546.

doi:10.1093/annonc/mdq299